Closed Form Characterization of Collision Free Velocities and Confidence Bounds for Non-holonomic robots in Uncertain Dynamic Environments

Bharath Gopalakrishnan[1*], Arun Kumar Singh [2*], K.Madhava Krishna[1]

***Abstract*— Navigating non-holonomic mobile robots in dynamic environments is challenging because it requires computing at each instant, the space of collision free velocities, characterized by a set of highly non-linear and non-convex inequalities. Moreover, uncertainty in obstacle trajectories further increases the complexity of the problem, as it now becomes imperative to relate the space of collision free velocities to a confidence measure. In this paper, we present a novel perspective towards analyzing and solving probabilistic collision avoidance constraints based on our previous works on *non-linear time scaling*. In particular, we have shown earlier that a time scaled version of collision cone constraints can be solved in closed form and thus can be used to efficiently characterize the space of collision free velocities.**

In the current proposed work, we present a probabilistic version of time scaled collision cone constraints obtained by representing obstacle states through generic probability distributions. We present a novel reformulation of the probabilistic constraints into a family of deterministic algebraic constraints. The solution space of each member of the family can be derived in closed form and at the same time, can also be related to the lower bound on confidence measure through Cantelli's inequality. Thus, the proposed work represents a significant improvement over the current state of the art frameworks where probabilistic collision avoidance constraints are solved through exhaustive sampling in the state-control space. We also present a cost metric which serves as the basis for the construction of the various collision avoidance maneuvers based on factors like deviation from the current path, acceleration/de-acceleration capability of the robot, confidence of collision avoidance etc. We very briefly explain how the current robot state can be connected to the solution space of safe velocities in smooth time optimal fashion. Finally, the validity of the proposed formulation is exhibited through extensive numerical simulation results.

I. Introduction

The problem of navigation in dynamic environments essentially boils down to that of computing the space of collision free velocities, at each control and sensing cycle. This is a challenging problem, specially for non-holonomic robots for which the space of collision free velocities are characterized by set of highly non-linear and non-convex inequalities. Moreover, in uncertain dynamic environments where obstacle trajectories cannot be known exactly, it is imperative to relate a particular solution space of collision free velocities to a confidence/risk measure. Previous approaches like [1], [2], [3], [4], [5] which tackled both these difficult aspects of navigation in uncertain dynamic environments, relied on exhaustive sampling in the state-control space. For example, [1] and [2] relied on checking a pre-defined set of velocities for the satisfaction of avoidance constraints modeled through velocity obstacle [6] concept. On the other hand [3] and [4] are based on Rapidly Exploring Random Trees [7] and thus have to perform sampling in the state space for collision avoidance. [5] performs sampling in the combined state-time space and thus, results in better avoidance maneuvers although at the cost of increased computation time. In this paper, we depart from these search based approaches and propose a framework for obtaining an analytical and closed form characterization of the solution space of collision free velocities and its associated confidence measure. We believe that the theoretical exposition presented here can serve as the basis for development of planners which will allow for replanning at each controller update, consequently leading to the realization of integrated planning and control frameworks for complex uncertain dynamic environments.

The proposed works is built on top of our recent formulations [8], [9] which provided an elegant methodology for characterizing the solution space of non-linear and non-convex collision avoidance constraints. These cited works introduced a concept called *time scaled collision cone* constraints which is a time scaled version of the collision cone constraints [10], used for characterizing avoidance maneuvers in dynamic environments. As shown in [9] *time scaled collision cone* constraints can be solved in closed form to obtain symbolic formulae characterizing the space of collision free velocities that the robot can attain along a given geometric path. Thus, evaluation of these symbolic formulae along multiple candidate paths/trajectories gives the complete characterization of the space of collision free velocities.

In the current work, we present a probabilistic version of the *time scaled collision cone* constraints, obtained by representing obstacle states through generic probability distributions. We derive symbolic form for the expectation and standard deviation of these probabilistic constraint functions and then use it to reformulate them to a family of deterministic algebraic constraints. The solution space of each member of the family can be derived in closed form and at the same time can be related to a lower bound on confidence measure. We also present a cost metric which serves as the basis for extracting various avoidance maneuvers from

∗ Equal contribution from first two authors [1] Robotics Research Center, IIIT-Hyderabad India, [2] Bio-Medical Robotics Lab, BGU, Israel arunkima@post.bgu.ac.il, bharath.gopalakrishnan@research.iiit.ac.in, mkrishna@iiit.ac.in. The research was partially supported by the Helmsley Charitable Trust through the Agricultural, Biological and Cognitive Robotics Initiative of Ben-Gurion University of Negev, Israel

the solution space based on factors like deviation from the current path, acceleration/de-acceleration capability of the robot, risk/confidence measure of collision avoidance etc.

The strength of the proposed work lies in the fact that it inherits the computational simplicity of our previous works [8], [9] and at the same time goes beyond them by introducing critical new insights which are essential for efficient navigation in uncertain dynamic environments. For example, [9] handles uncertainty in very deterministic manner. It samples obstacle trajectories from a specific region of trajectory distribution and ensures satisfaction of collision cone constraints with respect to each of these sampled trajectories. Important however is the fact that the constraints in [9] are exactly similar to what it would be in a standard deterministic setting. The probability of an obstacle trajectory plays no role in shaping of the constraints and as a consequence of this conservative approach, the solution space becomes highly restrictive as one samples from a larger portion of the obstacle trajectory distribution. As shown later, the current proposed work gets rid of this conservatism which allows us to obtain good solution space of collision free velocities even while incorporating less probable trajectories. Moreover, explicit consideration of probability of trajectories also forms the basis for associating each solution space to a measure of risk/confidence; a feature not present in [9]. At this juncture we would like to point out that approaches like [11] is in principal very similar to our previous work [9], in the sense that although they draw obstacle states from a distribution, the probability of each state plays no role in shaping of the constraints. Thus, the proposed work can also be seen as a theoretical advancement over existing works like [11].

The rest of this paper is organized as follows. Section II reviews the concepts from [9], specifically the concept of *time scaled collision cone* constraints and how it characterizes the solution space of collision free velocities in closed form. Section III introduces the probabilistic version of *time scaled collision cone* constraints and interleaves numerical simulation results alongside developing the theoretical framework for efficient solution of the probabilistic constraints. Section IV presents additional simulation results. The concluding remarks and a discussion on the future extension are provided in section V

II. Pre-Requisites: Time Scaled Collision Cone Constraints

The objective of this section is to first highlight how it is extremely challenging to solve the dynamic collision avoidance constraints for a non-holonomic robot. We then subsequently introduce *time scaled collision cone* constraints and show that it is indeed an efficient way of characterizing the solution space of non-linear and non-convex dynamic collision avoidance constraints.

Let the robot trajectory be represented as $\mathbf{X}^t = (x^t, y^t)^T$ with superscript "t" signifying the implicit dependency on time . Let t_o denote the time when the robot encounters collision with n obstacles. Further, let t_c denote the minimum of all the time instants by which the distance between the robot and of the obstacles becomes less than some safety threshold. The robot seeks to compute a trajectory which leads to a state $(x^{t_c}, y^{t_c}, \dot{x}^{t_c}, \dot{y}^{t_c})$ at time t_c which satisfies the following dynamic collision avoidance constraints.

$$f_i \geq 0, \forall i = 1, 2...n \tag{1}$$

$$f_i = (x^{t_c} - x_i^{t_c})^2 + (y^{t_c} - y_i^{t_c})^2 - R^2 - \frac{((\dot{x}^{t_c} - \dot{x}_i^{t_c})(x^{t_c} - x_i^{t_c}) + (\dot{y}^{t_c} - \dot{y}_i^{t_c})(y^{t_c} - y_i^{t_c}))^2}{(\dot{x}^{t_c} - \dot{x}_i^{t_c})^2 + (\dot{y}^{t_c} - \dot{y}_i^{t_c})^2}, \forall i = 1, 2...n \tag{2}$$

Set of inequalities (1) are called the collision cone constraints associated with each obstacle, wherein $x_i^{t_c}, \dot{x}_i^{t_c}$ and similar other terms are obstacle states at time t_c. f_i are called the collision cone function. As can be observed, collision cone constraints are differential constraints and thus needs to be solved along with the evolution model of the robot. For holonomic robots which have linear evolution models, the collision cone constraints takes (possibly non-convex) quadratic form. However, for non-linear evolution model associated with non-holonomic robots, these constraints become non-linear and non-convex.

As shown in [8], [9] an efficient approach to solve these complex collision cone constraints involves first obtaining a *time scaled* version of the constraints, the solution of which characterizes the space of collision free velocities that the robot can attain without altering the geometric path associated with its current trajectory. The *time scaled* version of the constraints can be solved in closed form to obtain a set of formulae, which can then be evaluated along multiple homotopic candidate trajectories to obtain the complete closed form characterization of the space of collision free velocities.

The *time scaled* version of the collision cone constraints can be obtained by changing the current time scale, t to the new time scale, τ in the trajectory definition $\mathbf{X}^t$. Such transformations do not alter the geometric path of the current trajectory but brings the following change in the velocity and acceleration profile.

$$\dot{\mathbf{X}}^\tau = \dot{\mathbf{X}}^t \frac{dt}{d\tau}, \ddot{\mathbf{X}}^\tau = \ddot{\mathbf{X}}^t (\frac{dt}{d\tau})^2 + \dot{\mathbf{X}}^t \frac{d^2t}{d\tau^2} \tag{3}$$

It is easy to understand from (3) that *time scaling* transformation results in change of velocities and accelerations through change in the temporal profile of the trajectory. In (3) $\frac{dt}{d\tau}$ is called the scaling function and decides the transformation between the time scales. By denoting $\frac{dt}{d\tau}(t_c) = s$ the set of velocities that the robot can attain at time t_c through scaling transformation can be denoted as $(s\dot{x}^{t_c}, s\dot{y}^{t_c})$. Thus, the *time scaled* version of collision cone constraints take the following form.

$$f_i^s \geq 0, \forall i = 1, 2...n \tag{4}$$

$$f_i^s = (x^{t_c} - x_i^{t_c})^2 + (y^{t_c} - y_i^{t_c})^2 - R^2 - \frac{((s\dot{x}^{t_c} - \dot{x}_i^{t_c})(x^{t_c} - x_i^{t_c}) + (s\dot{y}^{t_c} - \dot{y}_i^{t_c})(y^{t_c} - y_i^{t_c}))^2}{(s\dot{x}^{t_c} - \dot{x}_i^{t_c})^2 + (s\dot{y}^{t_c} - \dot{y}_i^{t_c})^2}, \forall i = 1, 2...n \tag{5}$$

As can be deduced from (4), *time scaled* collision cone constraints represents single variable quadratic inequalities in the form $a_i s^2 + b_i s + c_i \geq 0$. The symbolic formulae depicting the solution space of s are presented in [9].

The availability of these symbolic formulae allowed us in [9] to devise a brute force, conservative but computationally simple methodology for navigating in uncertain dynamic environments. It involved sampling from the obstacle trajectory distribution and enforcing collision avoidance constraints with respect to each of these samples. Although useful, the methodology did not explicitly exploit the information about probability associated with obstacle trajectories, which resulted in a conservative solution space. The next section is motivated towards relaxing the conservatism by explicitly exploiting the probability information of each obstacle trajectory.

III. Probabilistic Version of Time Scaled Collision Cone Constraints

In the scope of this paper, we consider uncertainty associated with evolution of obstacle trajectories. Considering the effect of robot uncertainty is a part of our future work and we give a brief preview of the possible approach towards the end of the paper. We assume that the i^{th} obstacle states at time t_c can be represented as a parametric probability distribution like Gaussian. For example, we adapt the Gaussian Process framework presented in [12], [13] and obtain the predicted obstacle states as Normal Distribution.

$$\begin{aligned} x_i^{t_c} &\sim N(\mu_i^x, \sigma_i^x), \dot{x}_i^{t_c} \sim N(\mu_i^{\dot{x}}, \sigma_i^{\dot{x}}) \\ y_i^{t_c} &\sim N(\mu_i^y, \sigma_i^y), \dot{y}_i^{t_c} \sim N(\mu_i^{\dot{y}}, \sigma_i^{\dot{y}}) \end{aligned} \tag{6}$$

In (6), μ_i^x, σ_i^x, $\mu_i^{\dot{x}}$, $\sigma_i^{\dot{x}}$ and similar others are mean and standard deviation associated with respective component of the predicted states of the i^{th} obstacle. With respect to (6), f_i^s now becomes a multivariate function of random variables and thus consequently a random variable itself. Thus, (4) can be interpreted a set of constraints on the possible outcome of the random variables f_i^s. Thus, satisfaction of constraints in this probabilistic scenario can be interpreted as a problem of maximizing ($Pr(f_i^s \geq 0)$). If the distribution of f_i^s is known in parametric form, then we can directly compute without much difficulty a value of s which maximizes $Pr(f_i^s \geq 0)$. However, the complicated non-linear nature of f_i^s prevents us from an obtaining any parametric form and thus we adopt an indirect approach towards our objective of maximizing $Pr(f_i^s \geq 0)$. Before we dwell on the details of our approach, we would like to point out that although the form of the distribution of f_i^s is not known, it is still possible to derive a closed form symbolic expression for the expectation and standard deviation of f_i^s in terms of variable s. As we will show shortly, this expressions hold the key to our proposed approach.

A. Expectation and Standard Deviation of f_i^s

The expectation of f_i^s is derived from the law of the unconscious statistician [14] which states that the expectation of a multivariate function g in terms of variable $z_1, z_2 ... z_n$ is given by the following expression

$$E[g(z_1, z_2 ... z_n)] = \int_{-\infty}^{\infty} ... \int_{-\infty}^{\infty} g(z_1, z_2 ... z_n) h(z_1, z_2 ... z_n) dz_1 dz_2 .. dz_n \tag{7}$$

Where $h(.)$ is the joint probability distribution of random variables. Thus, using (7), the expectation of f_i^s can be obtained in the following manner

$$E[f_i^s] = \mu_{f_i^s} = \int_{-\infty}^{\infty} \int_{-\infty}^{\infty} \int_{-\infty}^{\infty} \int_{-\infty}^{\infty} f_i^s(.) P_i(.) dx_i^{t_c} dy_i^{t_c} d\dot{x}_i^{t_c} d\dot{y}_i^{t_c} \tag{8}$$

Where $P_i(.)$ is the joint probability distribution of uncertain obstacles states $(x^{t_c}, y^{t_c}, \dot{x}^{t_c}, \dot{y}^{t_c})$. The above integral when computed symbolically through packages like MATHEMATICA [15] can be expressed in the following form

$$\mu_{f_i^s} = A_i s^2 + B_i s + C_i \tag{9}$$

Where $A_i(.)$, $B_i(.)$ and $C_i(.)$ are functions of the robot states and obstacle distribution parameters μ_i^1, σ_i^1, μ_i^2, σ_i^2 etc.

Similarly the standard deviation of the f_i^s when computed symbolically can be put in the following form

$$\sigma_{f_i^s} = \sqrt{E[(f_i^s - E[f_i^s])^2]} = \sqrt{D_i s^4 + E_i s^3 + F_i s^2 + G_i s + H_i} \tag{10}$$

We will now show that with the help of (9) and (10), it is possible to reformulate probabilistic constraints into a family of deterministic algebraic constraints. Each member of the family and its solution space can be related to a lower bound on $Pr(f_i^s \geq 0)$. Thus, we can seek to compute a solution space which empirically maximizes $Pr(f_i^s \geq 0)$.

B. Reformulating Probabilistic Constraints into Family of Algebraic Constraints

To understand the philosophy behind the reformulations presented in this section, consider figure 1 (a). Although the distribution of f_i^s is not known, we can still derive an expression for a strip of width $\mu_{f_i^s} \pm k\sigma_{f_i^s}$ with the help of the formulae for expectation and standard deviation derived in (9) and (10) respectively. It is straightforward to observe that the portion of the distribution covered by the strip would increase with the magnitude of the variable k. Now, recall that our objective is to maximize $Pr(f_i^s \geq 0)$. Alternatively speaking, we want to maximize the portion of the distribution of f_i^s that lies above/right of the zero line. As shown in figure 1 (b), this can be achieved by computing the solution space of the variable s with respect to the following family of constraints, for as large as possible value of k.

$$\mu_{f_i^s} \pm k\sigma_{f_i^s} \geq 0 \tag{11}$$

It is worth reiterating that as k increases, the width of the strip and consequently the part of the distribution of f_i^s which lie above/right of the "zero line" increases. This in turn would mean higher probability of $f_i^s > 0$. In fact as shown in the following lemma, it is possible to derive a lower bound on $Pr(f_i^s \geq 0)$, as a function of the variable k.

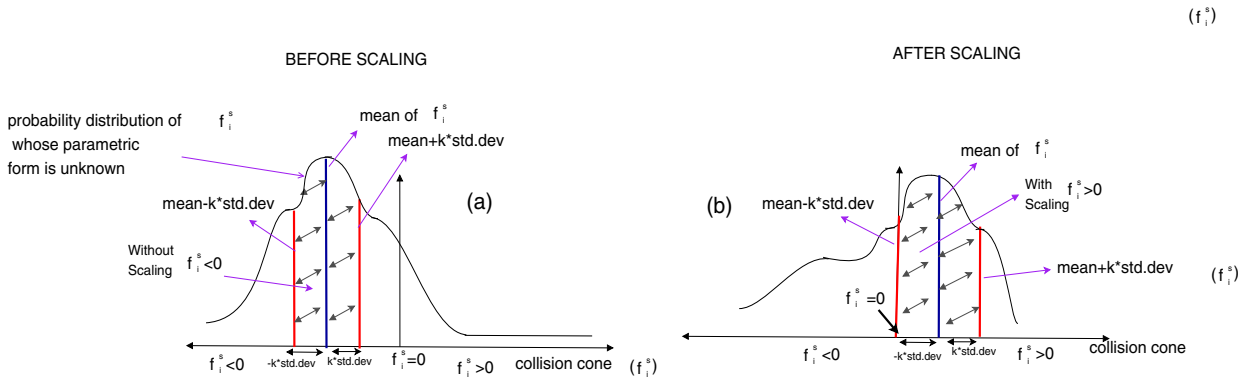

Fig. 1. In uncertain dynamic environments f_i^s are functions of random variable belonging to a particular distribution. The highly non-linear nature of f_i^s prevents us from obtaining an analytical parametric form for its probability distribution. A strip of width $\mu_{f_i^s} \pm k\sigma_{f_i^s}$ from the distribution of f_i^s is ensured to lies above zero through appropriate choice of variable s. As shown, in 13, the width of the strip as measured by the variable k has a direct correlation with the lower bound of $Pr(f_i^s \geq 0)$

Theorem 3.1: The lower bound on $Pr(f_i^s \geq 0)$ is given by $\frac{k^2}{1+k^2}$

Proof:

From Cantelli's inequality we have

$$Pr(f_i^s > \mu_{f_i^s} + k\sigma_{f_i^s}) \leq \frac{1}{1+k^2}, Pr(f_i^s > \mu_{f_i^s} - k\sigma_{f_i^s}) \geq \frac{k^2}{1+k^2} \tag{12}$$

Now, since $\mu_{f_i^s} - k\sigma_{f_i^s} \geq 0$ is ensured from (11), the following inequality holds

$$Pr(f_i^s > 0 \mid \mu_{f_i^s} - k\sigma_{f_i^s} > 0) \geq \frac{k^2}{1+k^2} \tag{13}$$

■

Based on the above discussions, it can be concluded that the (11) represents a family of deterministic algebraic constraints wherein the solution space of each family is related to a lower bound on $Pr(f_i^s \geq 0)$ through (13). Thus, solving (11) for a large value of k would improve the confidence measure or in other words reduce risk. However, as shown later as k increases, the solution space of s and consequently the space of velocities become highly restrictive. Thus, it is often required to make a trade-off between confidence/risks and ease of collision avoidance maneuvers.

We next derive the closed form characterization of the constraints (11).

C. Solving Inequalities (11)

Substituting (9) and (10) in (11) results in a quartic inequality in terms of variable s. Closed form solutions to these inequalities can be obtained without much difficulty. However, in this section we propose a simpler alternative approach based on the following quadratic approximation of the standard deviation, $\sigma_{f_i^s}$.

$$\sigma_{f_i^s} = \sigma_{f_i^{s^*}} + \sigma'_{f_i^{s^*}}(s - s^*) + \sigma''_{f_i^{s^*}} \frac{(s-s^*)^2}{2} \tag{14}$$

$$\sigma_{f_i^{s^*}} = D_i {s^*}^4 + E_i {s^*}^3 + F_i {s^*}^2 + G_i s^* + H_i$$
$$\sigma'_{f_i^{s^*}} = 4D_i {s^*}^3 + 3E_i {s^*}^2 + 2F_i s^* + G_i$$
$$\sigma''_{f_i^{s^*}} = 12D_i {s^*}^2 + 6E_i s^* + 2F_i$$

As can be observed from (14), that the quadratic approximation of $\sigma_{f_i^s}$ is obtained through Taylor series expansion around the variable s^*, which in turn is obtained by solving the following set of inequalities.

$$\mu_{f_i^{s^*}} \geq 0 \Rightarrow A_i {s^*}^2 + B_i s^* + C_i \geq 0 \tag{15}$$

It easy to appreciate that the solution to the above set of inequalities, s^* would correspond to avoiding the mean of the predicted obstacle states. Solving (15) is easy as it again represent single variable quadratic inequalities and thus, symbolic formulae depicting its solution space can be easily obtained. From the solution space, we choose s^* as the value closest to unity. The reasoning for this is simple and can be understood by recalling the time scaling equation (3). A s^* close to unity would imply minimum deviation from the temporal profile of the current trajectory. In other words, it would correspond to a collision avoiding velocity and acceleration which is very close to the ones that the robot would have reached while moving along the current trajectory.

Substituting (9) and (14) in (11), we get the following set of quadratic inequalities.

$$A_i s^2 + B_i s + C_i \pm k(\sigma_{f_i^{s^*}} + \sigma'_{f_i^{s^*}}(s - s^*) + \sigma''_{f_i^{s^*}} \frac{(s-s^*)^2}{2}) \geq 0 \tag{16}$$

Set of inequalities (16) represent the final form of the constraints in terms of mean and standard deviation for dynamic collision avoidance in uncertain dynamic environments. It is important to note that the structure of the constraints (16) is exactly same as that obtained in our previous works [8], [9]. Thus, as mentioned earlier, we explicitly include information of probability distribution of obstacle trajectories without incurring any additional computational costs. As can be seen, (16) are a set of single variable quadratic inequalities and thus a closed form characterization of its solution space can be easily obtained following the approach of [9].

In the next section, we describe some implementation examples, where among other things we also show that we incur very minimal error when moving from the original quartic polynomial inequalities to the quadratic approximation presented above.

D. Examples

The objective of this section is to validate the mathematical formulations discussed in the previous sections with the help of some numerical examples. The results presented in this section are obtained for the scenario where the robot encounters simultaneous collision with two obstacles. Due to space constraints, only a few results are discussed below. The readers are requested to follow the supplementary material for additional results [16]

Consider figures 2(a), 2(c), 2(e) and 2(g), where the curves shown in cyan corresponds to the samples of f_i^s. These are obtained by first drawing samples from the obstacle state distribution and then evaluating (4) with respect to these samples. The lines shown in blue are formed by the inequalities (16), which as discussed in the previous section, are a quadratic approximation of the strip $\mu_{f_i^s} \pm k\sigma_{f_i^s}$ from the distribution of f_i^s. It can be seen from the figures that as k increases from 1.2 to 2 , the area formed by the inequalities (16) increases and consequently it encompasses larger number of samples of f_i^s. Thus, it validates our proposition that satisfaction of (11) or equivalently (16), while increasing k would force larger portion of the distribution of f_i^s to be above/right of the "zero line", thereby increasing $Pr(f_i^s \geq 0)$ and the confidence of collision avoidance (reduction in colliding samples shown in yellow). Alternatively, improve in confidence with increase in k can also be inferred from figures 2(b), 2(d), 2(f), 2(h), where we evaluate the collision avoidance success through sampling. The samples shown in red are avoided while the robot collides with the samples shown in black. It is also worth pointing out that the $Pr(f_i^s \geq 0)$ estimated through sampling is generally more than that obtained based on the Cantelli's inequality (13). For example, for $k = 1.2$, the lower bound of $Pr(f_i^s \geq 0)$ obtained through (13) is 0.60 while that estimated from sampling is around 0.74. Similar observations can be made for $k = 2$ as well. Thus, this validates our claim that (13) indeed provides a lower bound on $Pr(f_i^s \geq 0)$.

The solution space of the variable s and consequently collision avoiding velocities are summarized in table I. It can be seen that the solution space shrinks with the increase in the k. In particular, it can be seen that the higher confidence maneuvers require robot to significantly decelerate ($s << 1$). Please note that the solution space shown in table I correspond to the velocities that the robot can attain without altering the current path. A more complete characterization of the solution space can be obtained by evaluating (16) over multiple candidate paths/trajectories. This is discussed in the next section.

E. Evaluating Solution Space of inequalities (16) along Multiple Candidate Trajectories

The simple structure of (16) allows us to easily evaluate it along multiple homotopic candidate trajectories and thus, obtain a more complete characterization of the solution space of collision avoiding velocities. Moreover, in some scenarios, solution space along the current trajectory could be null, in which case it becomes imperative to evaluate the solution space along other candidate trajectories. One such scenario is shown in figure 3. Various candidate trajectories are generated as a perturbation of the current trajectory, following the approach proposed in [9]. The solution space along the candidate trajectories are summarized in table II, table III and table IV. It can be seen that for a given k, the solution space improves with increase in deviation from the path associated with the current trajectory.

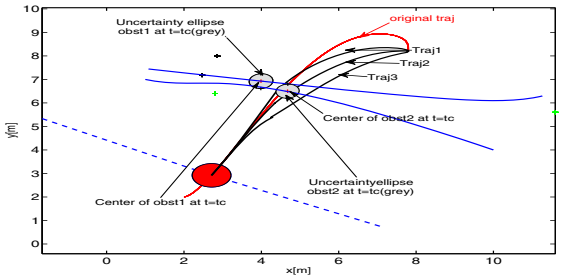

Fig. 3. A scenario where the solution space of inequalities (16) is null along the current trajectory. Thus, solution space of (16) is evaluated along multiple candidate trajectories, obtained as perturbations of the current trajectory. Among multiple solutions, one which minimizes the cost metric 17 is chosen

It is clear that multiple solution spaces corresponding to various $Pr(f_i^s > 0)$ (as measured by k) could exist for a given collision avoidance scenario. Thus, we propose the following cost metric for choosing a particular candidate trajectory and its associated solution space.

$$J_{cost} = w_1\Delta_t + w_2\Delta_p + w_3(1 - \frac{k^2}{1+k^2}) \tag{17}$$

The cost metric (17) has been adapted from our previous work [9] by adding the third term which accounts for the risk associated with a particular solution space (refer ineq. (13)). The remaining terms, Δ_t and Δ_p are the cost associated with changing the speed i.e accelerating or de-accelerating and changing the path respectively. w_1, w_2 and w_3 are the weights associated with the respective costs. A particular choice of weights extracts a particular collision avoidance maneuver from the solution space. For example, if minimizing risk and minimizing deviation from the current path are primary priorities, then w_2 and w_3 would be chosen much larger than w_1. For the scenario shown in figure 3, this would lead to the choice of the solution space associated with the candidate trajectory 2 for $k = 2$ (table III). Similarly, for a robot with limited acceleration/de-acceleration capability, w_1 and w_3 would be chosen much higher than w_2, which will consequently lead to the choice of solution space associated with candidate trajectory 3 for $k = 2$. Thus, various collision avoidance maneuvers can be extracted from the solution space, depending upon a particular collision scenario and actuation capabilities of the robot.

F. Connecting the Current State to the Solution Space in Smooth Time Optimal Fashion

The last two sections have shown how a collision avoidance maneuver can be characterized by choice of a candidate

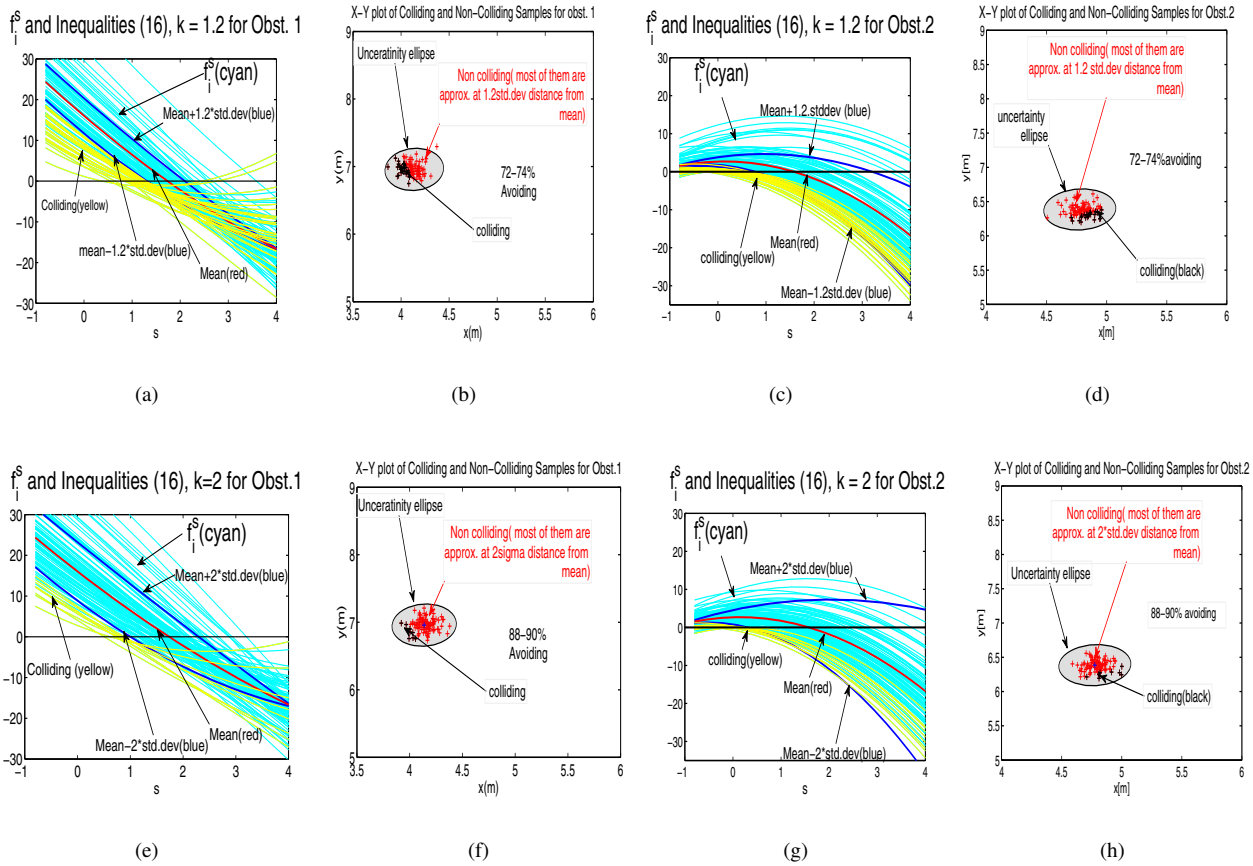

Fig. 2. Figures (a), (c), (e) and (g) provides validation of the mathematical formulation presented in section III. The plot lines shown in cyan denote the samples of f_i^s. The strip formed by the blue lines correspond to the sets of inequalities (16 and are a quadratic approximation of the strip $\mu_{f_i^s} \pm k\sigma_{f_i^s}$ from the distribution of f_i^s. It can be seen that the area formed by the inequalities (16 increases in direct proportion to k and consequently it encompasses more number of samples of f_i^s. Thus, enforcing (16) with increasing k leads to reduction in the number of colliding samples shown in yellow and improvement in $Pr(f_i^s \geq 0)$. It has also been shown in section III that (13) provides a lower bound on $Pr(f_i^s \geq 0)$ as a function of the variable k. We validate this claim through figures (b), (d), (f) and (h) where we empirically evaluate $Pr(f_i^s \geq 0)$ through sampling and show that it is always more than that obtained through (13). For example, consider figures (f) and (h) where for $k = 2$, we obtain $Pr(f_i^s \geq 0)$ as 0.90 through sampling, while that obtained from (13) is around 0.8

TABLE I

SOLUTION SPACE OF (16) FOR VARIOUS VALUES OF k

Obst. No	Sol.Space k = 1	Sol.Space k = 1.2	Sol.Space k = 1.5	Sol.Space k = 1.7	Sol.Space k = 2
Obst.1	[0 1.38] $\bigcup$ [18.45 ∞)	[0 1.3]	[0 1.18]	[0 1.11]	[0 0.9]
Obst.2	[0 0.8]	[0 0.69]	[0 0.53]	[0 0.43]	[0 0.33]
Resultant	[0 0.8]	[0 0.69]	[0 0.53]	[0 0.43]	[0 0.33]
Quadratic Approx. error	0.003	0.007	0.01	0.03	0.06

TABLE II

SOLUTION SPACE OF (16) ALONG THE CANDIDATE TRAJECTORY 1 FOR THE SCENARIO SHOWN IN FIGURE 3

Obst. No	Sol.Space k = 1	Sol.Space k = 1.2	Sol.Space k = 1.5	Sol.Space k = 1.7	Sol.Space k = 2
Obst.1	[0 0.82]	[0 0.73]	[0 0.61]	[0 0.52]	[0 0.39]
Obst.2	[0 0.26]	[0 0.2]	[0 0.13]	[0 0.0.07]	null
Resultant	[0 0.26]	[0 0.2]	[0 0.13]	[0 0.07]	null

TABLE III

SOLUTION SPACE OF (16) ALONG THE CANDIDATE TRAJECTORY 2 FOR THE SCENARIO SHOWN IN FIGURE 3

Obst. No	Sol.Space k = 1	Sol.Space k = 1.2	Sol.Space k = 1.5	Sol.Space k = 1.7	Sol.Space k = 2
Obst.1	[0 1.0]	[0 0.91]	[0 0.8]	[0 0.71]	[0 0.59]
Obst.2	[0 0.42]	[0 0.36]	[0 0.26]	[0 0.20]	[0 0.11]
Resultant	[0 0.42]	[0 0.36]	[0 0.26]	[0 0.20]	[0 0.11]

TABLE IV

SOLUTION SPACE OF (16) ALONG THE CANDIDATE TRAJECTORY 3 FOR THE SCENARIO SHOWN IN FIGURE 3

Obst. No	Sol.Space k = 1	Sol.Space k = 1.2	Sol.Space k = 1.5	Sol.Space k = 1.7	Sol.Space k = 2
Obst.1	[0 1.29]	[0 1.19]	[0 1.06]	[0 0.98]	[0 0.85]
Obst.2	[0 0.8]	[0 0.69]	[0 0.54]	[0 0.45]	[0 0.33]
Resultant	[0 0.8]	[0 0.69]	[0 0.54]	[0 0.45]	[0 0.33]

trajectory $\mathbf{X}^t$ and the solution space of the variable s. To connect the current state to the solution space one needs to compute a scaling function $\frac{dt}{d\tau}$ (refer 3) such that the following constraints are satisfied.

$$s_a \leq \frac{dt}{d\tau}(t_c) \leq s_b \tag{18}$$

s_a and s_b defines the boundary of the solution space of s. The profile of the scaling function before and after time t_c is free and hence we can utilize this redundancy to create a time optimal scaling function, subject to robot's velocity and acceleration bounds. In our earlier work [9], we have presented a sparse convex optimization based approach towards this objective. Here, we would like to point the readers towards our latest work [17] which can be easily adapted to reproduce the time optimal framework of [9], but with additional feature of acceleration continuity in the motion profile. This feature leads to smoother velocity profiles which can be tracked better.

IV. ADDITIONAL RESULTS AND DISCUSSIONS

In this section, we provide some additional implementation results and comparisons with our previous work [9].

A. Collision Avoidance with Discrete Probability of Obstacle States

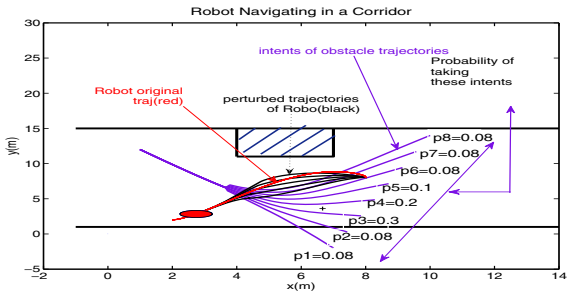

Fig. 4. A scenario where the obstacle states are predicted as discrete samples with associated probabilities. Even in this case, one could construct closed form expressions for expectation and standard deviation and consequently construct inequalities (16).

The derivation presented in the last section relied on the parametric form of the distribution of the obstacle states and the fact that we could obtain analytical functional form of expectation and standard deviation . However, one can easily obtain inequalities (16) even when the parametric form of the distribution is not known or is too complicated to allow for closed form derivation of expectation and standard deviation. In such scenarios one could use the framework proposed in [12] to represent predicted obstacle states as finite set of samples with associated probabilities. One can then proceed to compute the functional form of expectation and standard deviation in the following form.

$$E[f_i^s] = \mu_{f_i^s} = \sum \pi_i f_i^s \tag{19}$$

$$\sigma_{f_i^s} = \sqrt{\sum \pi_i {f_i^s}^2 - (\sum \pi_i f_i^s)^2} \tag{20}$$

Where, π_i is the probability associated with the i^{th} sample of predicted obstacle state. Similarly f_i^s is the *time scaled collision cone* constraint (4) in terms variable s for the i^{th} sample of predicted obstacle state.

As an implementation example, consider figure 4, which shows a robot and a dynamic obstacle navigating in a corridor like scenario. Eight samples with varying probabilities are used to predict obstacle states. It can be seen from the figure that the probabilities associated with each sample reflects the constraints posed by the restricted space in the corridor. Using (19) and (20), we construct inequalities (16) and solve it along the current and the perturbed trajectories shown in figure 4. The graphical representation of the solution process and the resulting collision avoidance are shown in figures 5(a)-5(d).

Consider figure 5(a) which shows various samples from the distribution of f_i^s and plot of inequalities (16) for $k = 0$. It is easy to deduce that solution space of (16) with $k = 0$ only ensures that $\mu_{f_i^s} > 0$ and as shown in figure 5(c), is not sufficient for collision avoidance with all the samples. The solution space corresponding to $\mu_{f_i^s} > 0$ results in collision with four of the predicted samples, along both the current and the best candidate trajectory. Thus, we gradually move to $k = 2$. It can be seen that similar to the results obtained with parametric distribution of obstacle states, with increase in k, the area formed by the inequalities (16) encompasses more samples of f_i^s and thereby improving $Pr(f_i^s > 0)$. The results for the intermediate values of k can be found in the supplementary material [16].

B. Comparison with Previous Work [9]

The objective of this section is to highlight how explicitly shaping the avoidance constraints through the probability of obstacle states, as proposed in section III leads to an improvement in the solution space. To this end, we compare the solution space obtained through the proposed formulation with that obtained through our previous work [9]. Before we explain the results, it is worth recalling that [9] draws obstacle states from a distribution but does not take into account the probability of the states. Further, the concept of variable k is only implicitly present in [9], in the sense that it signifies the portion of the distribution from which the obstacle states are drawn.

TABLE V

COMPARISON OF THE SOLUTION SPACE OBTAINED FROM THE PROPOSED FORMULATION AND PREVIOUS WORK [9]

Formulation	Sol.Space k = 1	Sol.Space k = 1.2	Sol.Space k = 1.5	Sol.Space k = 1.7	Sol.Space k = 2
[9]	[0 1.3]	[0 1.0]	[0 0.9]	[0 0.8]	[0 0.5]
Proposed	[0 1.96]	[0 1.18]	[0 1.056]	[0 0.964]	[0 0.811]

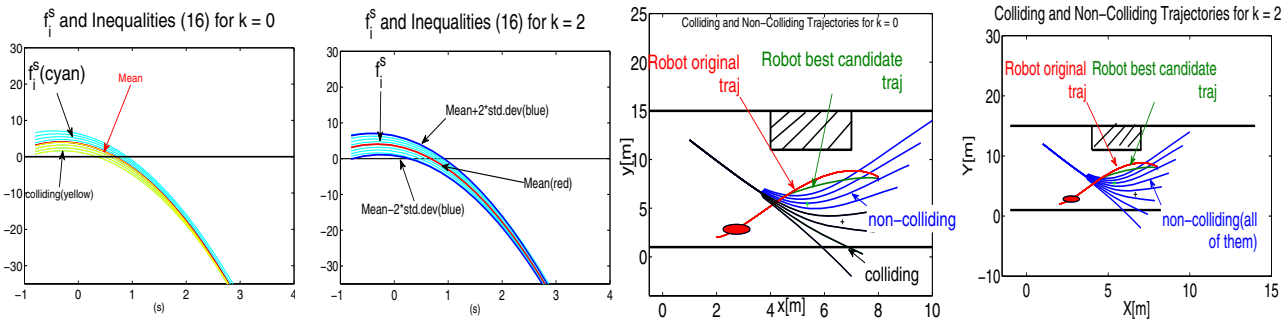

(a) (b) (c) (d)

Fig. 5. (a)-(b): Samples of f_i^s and inequalities (16) for $k = 0, 2$. It can be seen that $k = 0$ only ensures that the $\mu_{f_i^s} > 0$ and as shown in (c) is not sufficient for avoiding collisions with all the samples. Thus, k is gradually increased to 2. It can be seen from the figures (c) and (d) that as k increases, more number of obstacle samples are avoided.

Now coming to the results, we expect to obtain a conservative solution space with [9]. Table V validates this hypothesis. As can be seen, the proposed formulation consistently provides better solution space then [9]. Moreover, the difference/gap widens with increase in k. Physically, it means that in this particular case, a high confidence maneuver designed through [9] would require the robot to excessively slow down. In contrast, the proposed formulation would take into account the fact that some aggressive obstacle trajectories are less likely and thus, excessive de-acceleration is not required.

V. CONCLUSIONS AND FUTURE WORK

In this paper, we have shown that for a given distribution of obstacle states either in parametric or non-parametric form, it is possible to reformulate probabilistic collision avoidance constraints to a family of algebraic deterministic constraints. The solution space of each member of the family can be derived in closed form and at the same time can be related to a lower bound on confidence measure.

We are currently extending the current formulation to include robot's uncertainty. We have already observed that even while representing robot's state as random variables, we can still obtain symbolic expressions for expectation and standard deviation of f_i^s in a form similar to that presented in (9) and (10). Thus, the entire formulation of section III can be very easily adapted to include robot's uncertainty information.

REFERENCES

[1] Kluge, B., and Prassler, E. (2006, January). Recursive probabilistic velocity obstacles for reflective navigation. In Field and Service Robotics (pp. 71-79). Springer Berlin Heidelberg.

[2] Kim, S., Guy, S. J., Liu, W., Wilkie, D., Lau, R. W., Lin, M. C., and Manocha, D. Predicting Pedestrian Trajectories for Robot Navigation. In Proc. of the workshop Crossing the Reality Gap: Control, Human Interaction and Cloud Technology for Multi- and Many- Robot Systems 2014 IEEE ICRA 2014. Hong Kong, China, May 31 - June 7, 2014

[3] Fulgenzi, C., Tay, C., Spalanzani, A., and Laugier, C. (2008, September). Probabilistic navigation in dynamic environment using rapidly-exploring random trees and gaussian processes. In Proc. IEEE IROS 2008 (pp. 1056-1062).

[4] Rios-Martinez, J., Spalanzani, A., and Laugier, C. (2011). Probabilistic autonomous navigation using risk-rrt approach and models of human interaction. In Proc. IEEE IROS 2011 .

[5] Kushleyev, A., and Likhachev, M. Time-bounded lattice for efficient planning in dynamic environments. In Proc. of IEEE ICRA 2009 (pp. 1662-1668).

[6] Fiorini, P., and Shiller, Z. (1998). Motion planning in dynamic environments using velocity obstacles. IJRR, 17(7), 760-772.

[7] Lavalle, S. M. (1998). Rapidly-Exploring Random Trees: A New Tool for Path Planning.

[8] Singh, A. K., and Krishna, K. M. (2013, December). Reactive collision avoidance for multiple robots by non linear time scaling. In Proc. of IEEE CDC 2013 (pp. 952-958).

[9] Gopalakrishnan, B., Singh, A. K., and Krishna, K. M. (2014, September). Time scaled collision cone based trajectory optimization approach for reactive planning in dynamic environments. In Proc. of IEEE IROS 2014 (pp. 4169-4176).

[10] Chakravarthy, A., and Ghose, D. (1998). Obstacle avoidance in a dynamic environment: A collision cone approach. Systems, Man and Cybernetics, Part A: Systems and Humans, IEEE Transactions on, 28(5), 562-574.

[11] Snape, J., van den Berg, J., Guy, S. J., and Manocha, D. (2011). The hybrid reciprocal velocity obstacle. Robotics, IEEE Transactions on, 27(4), 696-706.

[12] Joseph, J. M., Doshi-Velez, F., and Roy, N. (2010, May). A Bayesian Nonparametric Approach to Modeling Mobility Patterns. In Twenty-Fourth AAAI Conference on Artificial Intelligence.

[13] Ko, J., and Fox, D. (2009). GP-BayesFilters: Bayesian filtering using Gaussian process prediction and observation models. Autonomous Robots, 27(1), 75-90.

[14] Papoulis, A. (1984), Probability, Random Variables, and Stochastic Processes, New York: McGraw-Hill, p. pp. 139152

[15] Wolfram, S. (2009). Mathematica. Wolfram Research, Champaign.

[16] Efficient Computation of the Space of Safe Velocities for Non-Holonomic Robots in Uncertain Dynamic Environments, Arun Kumar Singh,K. Madhava Krishna, February 2015. Report no: IIIT/TR/2015/3.(pdf)

[17] Singh, A. K., Gopalakrishnan, B., and Krishna, K. M. Time Optimal Control along Specified Paths with Acceleration Continuity: A Non-Linear Time Scaling based approach. In Proc. of Indian Control Conference 2015 (pp.353-359)